THE JOURNAL OF PHYSICAL CHEMISTRY B

ARTICLE

pubs.acs.org/JPCB

Monte Carlo Studies of the XY Model on Two-Dimensional Curved Surfaces

Robin L. Blumberg Selinger,*[,†] Andrew Konya,[†] Alex Travesset,[‡] and Jonathan V. Selinger[†]

[†]Liquid Crystal Institute, Kent State University, Kent, Ohio 44242, United States

[‡]Department of Physics and Astronomy and Ames Laboratory, Iowa State University, Ames, Iowa 50011, United States

ABSTRACT: To explore the interaction between topological defects and curvature in materials with orientational order, we perform Monte Carlo studies of the two-dimensional XY model on the surface of curved substrates. Each curved surface is patterned with a random lattice constructed via random sequential absorption, and an XY spin is positioned at each lattice site. Spins lie in the plane locally tangent to the surface and interact with neighbors defined via a distance cutoff. We demonstrate that the relative phase associated with vortices is significant in curved geometries and plays a role in microstructural evolution. We also observe that any nonuniform curvature, e.g., on the surface of a torus, induces spontaneous segregation of positive and negative vortices and promotes the formation of deeply metastable defect microstructures. Though qualitative in nature, these observations provide novel insights into the patterning of topological defects in curved geometries and suggest that the Kosterlitz−Thouless transition may be altered in geometries with nonuniform curvature.

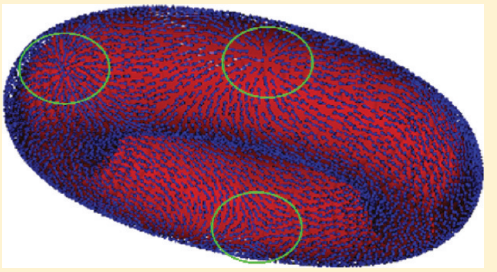

INTRODUCTION

Critical phenomena and phase transitions in two dimensions have inspired many theoretical physics studies over the years, including pioneering work by H. Eugene Stanley in 1966.[1] Recently, a major theme of theoretical research in condensed-matter physics has been the complex interaction of geometry with orientational order and topological defects. For an orientationally ordered achiral material in a simple, flat geometry, the free energy generally favors a microstructure with long-range orientational order. The imposition of curvature on an orientationally ordered material can produce geometrical frustration, thus disrupting the long-range order present in flat crystals. This geometrical frustration was noted in early influential work on hexatic and crystalline order in membranes by Nelson and Peliti.[2]

Since then, related phenomena have been investigated in a wide range of models by many theorists, as discussed in reviews.[3−5] This body of research has relied on the mathematical formalism of differential geometry to describe couplings between curvature and orientational order that are required by geometrical considerations.[6] A key finding of these studies is that in many materials, orientational order in a thin film is energetically coupled to the film's local curvature. Topological defects with a positive or negative charge are attracted to regions of positive or negative Gaussian curvature, respectively.

One way to explore this behavior is through the study of the classical two-dimensional (2-d) XY model, which displays topological defects, known as vortices, with a charge of ±1. Below the Kosterlitz−Thouless transition temperature in a flat 2-d system, the XY model shows quasi-long-range orientational order and vortices arise only as thermally activated excitations. However, on a closed surface, as required by the Gauss−Bonnet Theorem, the net topological charge must be $2 - 2g$, where g is the genus of the shape, or the number of "handles" it has. For example, a sphere has $g = 0$ and a net topological charge of +2. Thus, for an XY model on a sphere, the equilibrium defect density must be nonzero even at zero temperature, a classic example of how topology induces geometric frustration. Previous theoretical studies have investigated the effect of orientational order on a sphere,[7−9] a torus,[10] and more general topographies.[11]

In this paper, we describe Monte Carlo simulation studies of the 2-d XY model on a variety of curved surfaces. This model describes defects in a single layer film of liquid crystal in the Smectic C phase on a curved rigid substrate, where the XY spin represents the local molecular tilt orientation. The model also describes the tilt field in a Langmuir film of lipids confined on the surface of a liquid droplet, in the limit where the droplet shape is determined only by surface tension and is essentially unaffected by film microstructure.

By annealing an XY model system from an initially disordered state on various curved surfaces, we explore the details of evolving defect-rich microstructures, including the formation of deeply metastable states. We present results for simulation studies of the XY model on a sphere, a torus, and an "egg-crate" surface of height $z = A \sin kx \sin ky$. From these studies, we derive new insight into the evolution and patterning of defects in

Special Issue: H. Eugene Stanley Festschrift

Received: June 20, 2009
Revised: September 19, 2011
Published: October 04, 2011

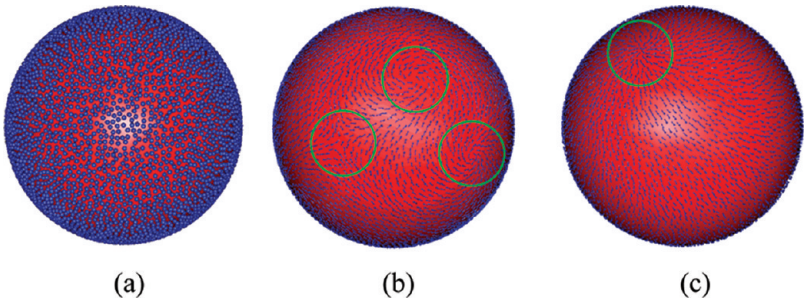

Figure 1. (a) A random lattice on a sphere is constructed via random sequential absorption. (b) An XY model on the random lattice is partially annealed, showing +/− vortices with a net topological charge of +2. (c) When annealing is complete, two +1 vortices remain at opposite poles.

curved geometries and the formation of deeply metastable microstructures.

SIMULATION MODEL

The classical 2-d XY model describes the energy of an array of vector spins, e.g., in a square lattice with nearest neighbor interactions.

$$H = -J \sum_{\langle i,j \rangle} (\mathbf{s}_i \cdot \mathbf{s}_j) \quad (1)$$

To map the XY model onto a curved substrate of arbitrary shape, we position the spins on a random lattice constructed via 2-d random sequential absorption (RSA).[12] On a flat plane, RSA is carried out via random deposition of disks, e.g., like gluing pennies on a table, until saturation is achieved, with the rule that each random deposition step is rejected if it produces overlap with any previously deposited disk. RSA produces a disordered lattice with short-range positional order. To generalize this procedure to a curved 2-d substrate such as the surface of a torus, we instead deposit small spheres (small compared to the surface's radii of curvature) with their centers located on the curved surface. In the random deposition process, we take account of the surface's metric to ensure that the deposition attempt rate per unit area is uniform. Saturation may be defined, e.g., as no further successful depositions after an arbitrary number of failed attempts. The centers of the deposited particles represent the sites in a random lattice.

Once this disordered structure is produced, we place an XY spin $\mathbf{s}_i$ at each lattice site i. Each spin has a unit length and one angular degree of freedom and is confined to the plane locally tangent to the curved surface. We allow interactions as defined in eq 1 between any pair of spins whose separation is less than a cutoff distance, r_{cut}. In a curved geometry, neighboring spins are in general not coplanar, and the dot product from eq 1 is calculated in three dimensions. Spins, $\mathbf{s}_i$, are initially random and evolve via Monte Carlo simulation. This model is quite similar in approach to the coarse-grained model used by Shin et al[13] to study defect structures in a nematic thin film on a sphere.

This random lattice XY model produces a disordered energy landscape for topological defects, even on a flat substrate, as the core energy of a vortex or antivortex varies with position. Thus, even without adding an explicit pinning term to the Hamiltonian in eq 1, a vortex is subject to an effective random pinning potential associated with heterogeneity of the random lattice. Increasing the value of r_{cut} partially smooths out this heterogeneity. By contrast, a regular square or triangular lattice produces a simpler energy landscape for defects, with a regular array of equivalent local minima located at the center of each unit cell.

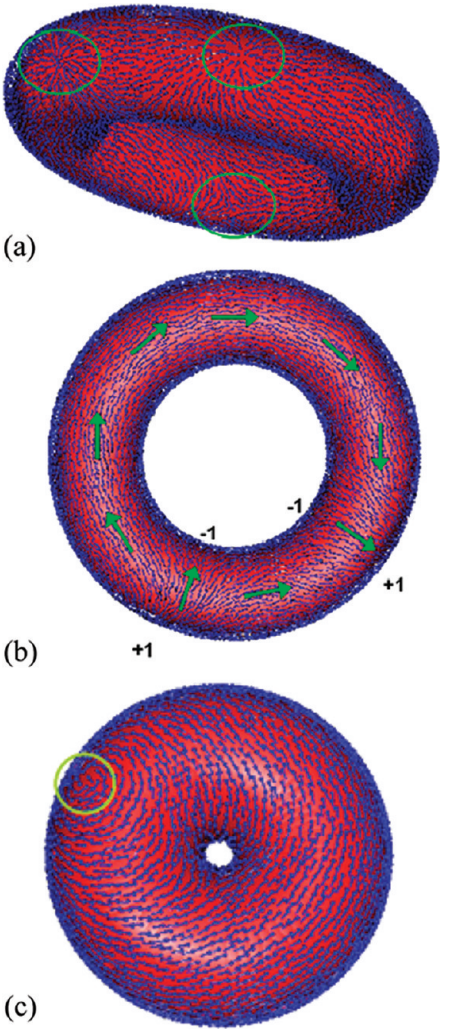

Figure 2. Monte Carlo study of the XY model on a torus. (a) During annealing, positive vortices segregate to the outer surface of the torus with an aspect ratio of 3 where Gaussian curvature is positive, while negative vortices segregate to the inner surface where Gaussian curvature is negative. (b) Deeply metastable microstructure with two domains separated by boundaries composed of a pair of +/− vortices. Because the number of domains must be even, the number of defects in this geometry is zero or a multiple of four, with zero net topological charge. (c) A torus with aspect ratio $r = 1.2$ shows defects even when well annealed.

The mobility of topological defects in the XY model also depends on the geometry of the underlying lattice. To move from one local minimum to another, a vortex must go over an energy barrier that is a close analog of the Peierls barrier for dislocation motion in crystals.[14] The height of this energy barrier for defect motion is sensitive to both lattice structure and orientation. In a square or triangular lattice, defects move easily with a low energy barrier along symmetric lattice directions but have lower mobility in other directions, just as screw dislocations in a crystal have higher mobility along certain lattice planes. In a disordered spin−lattice, vortex mobility is locally heterogeneous but statistically isotropic.

In Figure 1a, we show a sphere decorated with an RSA-generated random lattice of points. In Figure 1b, we show the XY model mapped onto the surface, partially annealed, and observe that extra +/− pairs are present. When the annealing process is complete, the extra defects pair-annihilate, leaving only two +1 vortices as required by the Gauss−Bonnet theorem. Because of mutual repulsion, they move to opposite poles, and only one of them is visible in Figure 1c.

On a flat substrate, the energy of a vortex is invariant under the addition of any arbitrary constant, or "phase", to the angular orientation of every spin in the system. However, on a curved surface, we note that the energy of a vortex depends sensitively on its phase. As shown in Figure 1c, in the annealed state, the phase for a +1 defect is such that spins point either toward or away from the defect core. On a spherical surface, this phase dependence of the energy is an artifact of the coarseness of the random lattice, which depends on the size of the spheres deposited in the RSA algorithm. The spins surrounding the defect core essentially define a cone whose opening angle depends on their average spacing. They are more nearly parallel and subtend a total angle less than 2π if they point toward or away from the tip of the cone, rather than around it.

Next, we consider the XY model mapped onto a torus with major radius $R_1 = 3$ and minor radius $R_2 = 1$. With genus $g = 1$, the torus has a net topological charge density of zero; in the defect-free ground state, all spins point either clockwise or counter-clockwise with respect to the central axis.

This defect-free equilibrium state is not always found via Monte Carlo simulation. When annealed from a disordered initial state, +1 vortices segregate to the outer surface of the torus, where Gaussian curvature is positive, and −1 vortices segregate to the inner surface, where Gaussian curvature is negative, as shown in Figure 2a, demonstrating that curvature indeed acts as an external potential for defects. As a result, defect pair annihilation is inhibited, and the system may not reach the defect-free ground state via annealing. At temperatures near zero, the resulting microstructure shows an even number of domains of alternating spin orientation. Each boundary separating clockwise and counter-clockwise oriented domains contains one +/− vortex pair arranged with the −1 vortex on the inner surface and the +1 vortex on the outer surface, as shown in Figure 2b.

Because topology dictates that the number of boundaries separating clockwise/counter-clockwise domains must be even, the net number of topological defects on the torus at low temperature is thus a multiple of 4. The resulting microstructure is deeply metastable, as defect pair annihilation is strongly inhibited by defect segregation to inner and outer surfaces. Likewise, the energy barrier for annihilation of two neighboring domain boundaries is high because a total of four defects must disappear via double pair-annihilation.

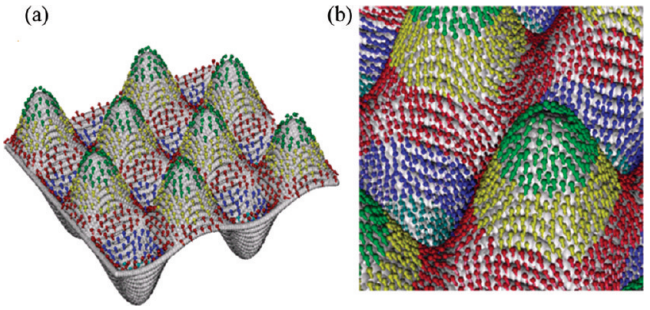

Figure 3. XY model on an "egg-crate" surface, with spins color-coded by height. (a) At low temperature, positive vortices are found at each point of maximum/minimum height and negative vortices at each saddle point, with zero net topological charge. (b) Detailed view for a denser random lattice system.

One might expect that strong repulsion between domain boundaries would result in their migration to opposite sides of the torus, just as like-signed vortices repel on the sphere. However, we observe that domain boundaries do not experience mutual repulsion except at close range, indicating that the associated "stress field" of a domain boundary drops off rapidly over a distance comparable to the spacing of its constituent defects, just as in grain boundaries in metals.

The origin of the topological defects on the torus is strongly suggestive of high activation barriers. In ref 10, it was shown that the ground state of a torus contains defects only for a maximum number of particles, M_c,

$$M < M_c \equiv \exp\left(\frac{-36E_{\text{core}}}{K_A}\right)\left(\frac{r+1}{r-1}\right)^6 \qquad (2)$$

where E_{core} is the core energy of the defect, K_A is the stiffness constant, and r is the aspect radius of the torus. It is therefore predicted that only for extremely fat torus, $r \sim 1$, stable topological defects should be expected in equilibrium; such a structure is shown in Figure 2c. The abundance of topological defects in the XY model on the torus is therefore indicative of high activation barriers to equilibrium, which are physically relevant and should be observed in experiments. The gradient in curvature serves as a kind of external field that aligns and separates thermally activated vortex pairs. We leave this issue for future investigation.

Next, we consider the arrangement of topological defects on an "egg-crate" surface of the form $z = A \sin kx \sin ky$, with periodic boundary conditions so that the net topological charge must be zero. As shown in Figure 3a,b, we find a +1 vortex at each point of maximum and minimum height, and a −1 defect at each saddle point.

Defect "phase" plays an important role in this system, giving rise to two degenerate equilibrium microstructures. In one, positive vortices have phase such that spins point toward the defect core at every point of maximum height and away from the defect core at every minimum; in the other degenerate state, those phases are reversed. Thus, under annealing, a large system will typically show domain structures where different regions of the system have fallen into one or the other of these degenerate states. Such a microstructure is shown in Figure 3b, where neighboring peaks (in the back row) have vortices of opposite phase.

If we further refine the spacing of the random lattice relative to the length scale defined by the spatial periodicity of $2\pi/k$, eventually we find a system whose ground state is defect-free.

For this reason, we expect that a thin film of Smectic C liquid crystal on a rigid egg-crate substrate may not, in general, produce a defect-rich microstructure when annealed from a disordered state. However, it is interesting to consider whether the presence of substrate curvature will nevertheless affect the system at finite temperature. For instance, the Kosterlitz−Thouless transition may be affected by substrate shape, as gradients of curvature favor the nucleation and separation of thermally activated vortex pairs. Again, we leave this issue for future investigation.

INTRINSIC AND EXTRINSIC CURVATURE

To analyze the simulation results, it is useful to interpret the energy of eq 1 in terms of the concepts of intrinsic and extrinsic curvature from differential geometry. For this purpose, we take the continuum limit of the lattice Hamiltonian as

$$H = \int \sqrt{g} d^2x \left[\frac{1}{2} K_A (\nabla \mathbf{s})^2\right] \tag{3}$$

where $\nabla \mathbf{s}$ is the three-dimensional (3-d) gradient of the continuous vector field $\mathbf{s}(\mathbf{x})$ and $\sqrt{g}d^2x$ is the measure of integration for the surface. The coefficient K_A is the elastic coefficient for orientational order on the surface, analogous to the Frank constant of a nematic liquid crystal. It should have the same order of magnitude as the lattice coefficient J in eq 1.

We now write the vector field $\mathbf{s}(\mathbf{x})$ in terms of an angle $\theta(\mathbf{x})$,

$$\mathbf{s}(\mathbf{x}) = \mathbf{t}_1(\mathbf{x}) \cos \theta(\mathbf{x}) + \mathbf{t}_2(\mathbf{x}) \sin \theta(\mathbf{x}) \tag{4}$$

where $\mathbf{t}_1(\mathbf{x})$ and $\mathbf{t}_2(\boldsymbol{x})$ are an orthonormal basis for the local tangent plane. The basis vectors $\mathbf{t}_1$ and $\mathbf{t}_2$ and the angle θ all depend on position, so they all contribute to the gradient. Through some algebraic manipulation, the 3-d interaction of eq 3 can be simplified into the sum of two terms,

$$H = \int \sqrt{g} d^2x \left[\frac{1}{2} K_A (\nabla\theta + \mathbf{A})^2 + \frac{1}{2} K_A (\mathbf{s}\cdot\mathbf{K}\cdot\mathbf{K}\cdot\mathbf{s})\right] \tag{5}$$

Here, the first term is the *intrinsic* coupling between XY order and curvature, which was originally derived by Nelson and Peliti[2] on the basis of a 2-d covariant derivative coupling $g^{\mu\nu} D_\mu\theta D_\nu\theta$, which compares the vector field at different positions on the surface through parallel transport. As they pointed out, the vector field $\mathbf{A}$ is a vector potential, which expresses the geometrical frustration of XY order due to Gaussian curvature. It satisfies $\nabla \times \mathbf{A} = -K$, where K is the Gaussian curvature of the surface. The second term is the *extrinsic* coupling between XY order and the curvature tensor $\mathbf{K}$. It gives a favored alignment of the absolute orientation of the vector field, with respect to the 3-d curvature direction. In that sense, it is analogous to an electric field acting on the director of a nematic liquid crystal. A related analysis of these couplings has been done by Jiang et al.[15]

The distinct effects of the intrinsic and extrinsic couplings can be seen by considering three special geometries:

(1) *Cylinder*: The Gaussian curvature of a cylinder is zero, so the XY order is not frustrated and does not need to develop defects. In the intrinsic coupling term, the vector potential $\mathbf{A}$ is zero, and hence the intrinsic coupling only favors a simple uniform ground state with constant θ. The most important physics comes from the extrinsic coupling term, which breaks the rotational symmetry in the local tangent plane and favors a particular orientation of the XY order, which is along the cylinder axis. This curvature-induced alignment makes sense because the interaction of eq 1 treats the $\mathbf{s}_i$ as 3-d vectors: they are parallel vectors in 3-d if they are aligned along the cylinder axis but not if they are aligned around the cylinder's circumference. The strength of the aligning potential is proportional to two powers of the curvature tensor $\mathbf{K}$ and hence to $1/r^2$, where r is the radius of the cylinder.

(2) *Sphere*: The most important physics for a sphere comes from the intrinsic coupling. In this term, the vector potential $\mathbf{A}$ is nonzero, and it shows the effect of the Gaussian curvature on the XY order. By contrast, the extrinsic coupling is unimportant because the curvature tensor $\mathbf{K}$ is isotropic in the local tangent plane, proportional to the identity tensor, and hence the extrinsic coupling term is a constant. (The sphere simulations described in the previous section do not perfectly fit this description because the lattice spacing is not negligible compared with the sphere radius. On the length scale of the lattice spacing around a defect, the sphere resembles a cone, with a slight extrinsic aligning potential acting on the XY order. That is the reason why the energy depends on the "phase" of the defect.)

(3) *Torus*: For a torus, both the intrinsic and extrinsic couplings are important. The intrinsic coupling responds to the Gaussian curvature of the torus, favoring positive topological defects on the outer surface where the Gaussian curvature is positive and negative topological defects on the inner surface where the Gaussian curvature is negative. The extrinsic coupling favors alignment of the XY order running the long way around the torus. To reduce the extrinsic coupling, any regions where the XY order is in disfavored directions are squeezed into narrow domain walls, with a wall width of the order of the minor radius of the torus. This mechanism explains the domain structure seen in the Monte Carlo simulations of the torus.

Note that the simple 3-d dot-product interaction of eq 1 leads to intrinsic and extrinsic couplings with *equal coefficients*. Of course, there is no fundamental reason why these coefficients must be equal; they depend on the microscopic interaction. In experimental systems, the interaction may well be more complex than this simple dot product. However, any 3-d interaction between the orientations of neighboring molecules should contribute to both the intrinsic and extrinsic couplings. Thus, we expect that these two coefficients should have the same order of magnitude. There is no reason to neglect either of these couplings. Both intrinsic and extrinsic couplings should be important in understanding the textures in any system with curvature and orientational order.

DISCUSSION

In this work, we have considered the case of an XY model on a rigid substrate and examined the dynamics and patterning of defects in response to the substrate's curvature. In other systems, this energetic coupling between defects and curvature works in the opposite sense: the presence of fixed defects in an orientationally ordered material induces changes in curvature. For instance, in a nematic liquid crystal elastomer (LCE), a topological defect in the director field of a thin film may be fixed in place via cross-linking. On heating or cooling, the defect induces the formation of curvature; a positive topological defect induces the formation of positive Gaussian curvature, whereas a negative

defect induces negative Gaussian curvature. Warner and co-workers[16] have proposed to exploit this behavior by patterning the director field in flat LCE films such that it folds into any desired 3-d shape upon heating or cooling.

In lipid vesicles in the tilted "gel" phase, we again expect that defects in the tilt field of the lipid membrane will be coupled energetically with the vesicle's local curvature. However, in contrast to our XY model simulations, which were fixed on a rigid substrate, and to the liquid crystal elastomers where the director field is fixed in the body frame of the material, tilted lipid membranes allow a potentially richer set of pattern evolution phenomena as *both the membrane shape and its tilt field* coevolve in time.

Static equilibrium states in such systems have already been studied theoretically (see, e.g., ref 15 and references therein). However, kinetic effects may allow such systems to become trapped in metastable states due to the competing kinetics of defect migration/annihilation and overall vesicle shape evolution. Topological defects may induce the formation of membrane curvature, which in turn inhibits their mobility and prevents pair annihilation. In such a system, we expect a rich variety of pattern formation and shape evolution, e.g., when an initially spherical lipid vesicle is quenched from the untilted liquid crystal phase into the tilted gel phase. Indeed, Hirst and co-workers[17] have observed this type of unusual shape evolution in lipid vesicles of dipalmitoyl phosphatidylcholine (DPPC) giving rise to disordered structures. We are currently pursuing coarse-grained simulation models of this phenomenon in order to explore the competition between the kinetics of defect motion and shape evolution in vesicles and the resulting pattern formation.

AUTHOR INFORMATION

Corresponding Author

*E-mail: rselinge@kent.edu.

ACKNOWLEDGMENT

This work is supported by NSF-DMR-0605889 and NSF-DMR-0748475 and the Branches Cost Sharing Fund of the Institute for Complex Adaptive Matter.

REFERENCES

(1) Stanley, H. E.; Kaplan, T. A. *Phys. Rev. Lett.* **1966**, *17*, 913–916.
(2) Nelson, D. R.; Peliti, L. *J. Phys. (Paris)* **1987**, *48*, 1085–1092.
(3) Bowick, M. J.; Travesset, A. *Phys. Rep.* **2001**, *344*, 255–308.
(4) Nelson, D. R., *Defects and Geometry In Condensed Matter Physics*; Cambridge University Press: Cambridge, U.K., 2002.
(5) Turner, A. M.; Vitelli, V.; Nelson, D. R. *Rev. Mod. Phys.* **2010**, *82*, 1301–1348.
(6) Kamien, R. D. *Rev. Mod. Phys.* **2002**, *74*, 953–971.
(7) Mackintosh, F. C.; Lubensky, T. C. *Phys. Rev. Lett.* **1991**, *67*, 1169.
(8) Evans, R. M. *J. Phys. II* **1995**, *5*, 507.
(9) Lenz, P.; Nelson, D. *Phys. Rev. E: Stat., Nonlinear, Soft Matter Phys.* **2003**, *67*, 31502.
(10) Bowick, M.; Nelson, D.; Travesset, A. *Phys. Rev. E: Stat., Nonlinear, Soft Matter Phys.* **2004**, *69*, 41102.
(11) Vitelli, V.; Nelson, D. *Phys. Rev. E: Stat., Nonlinear, Soft Matter Phys.* **2004**, *70*, 051105.
(12) Feder, J. *J. Theor. Biol.* **1980**, *87*, 237.
(13) Shin, H.; Bowick, M. J.; Xing, X. *Phys. Rev. Lett.* **2008**, *101*, 037802.
(14) Selinger, R. L. B.; Smith, B. B.; Luo, W.-D. *MRS Proc.* **2000**, *653*, Z5.4.1. See also **arXiv:cond-mat/0012447**.
(15) Jiang, H.; Huber, G.; Pelcovits, R.; Powers, T. R. *Phys. Rev. E: Stat., Nonlinear, Soft Matter Phys.* **2007**, *76*, 031908.
(16) Modes, C. D.; Bhattacharya, K.; Warner, M. *Phys. Rev. E: Stat., Nonlinear, Soft Matter Phys.* **2010**, *81*, 060701.
(17) Hirst, L.; Ossowski, A.; Fraser, M. Understanding crumpling lipid vesicles at the gel phase transition. APS March Meeting 2011, Dallas, TX, March 21−25, 2011; *Bulletin of the American Physiological Society*; Vol 56, No. 1; http://meetings.aps.org/link/BAPS.2011.MAR.L9.6.